Carbohydrate Polymers 102 (2014) 238–245

Contents lists available at ScienceDirect

Carbohydrate Polymers

journal homepage: www.elsevier.com/locate/carbpol

Preparation, characterization and cytotoxicity of schizophyllan/silver nanoparticle composite

A.M. Abdel-Mohsen[a,g,*], Rasha M. Abdel-Rahman[c], Moustafa M.G. Fouda[b,g,**], L. Vojtova[a], L. Uhrova[d], A.F. Hassan[e], Salem S. Al-Deyab[b], Ibrahim E. El-Shamy[f], J. Jancar[a,d]

[a] Central European Institute of Technology (CEITEC), Brno University of Technology, Brno Czech Republic
[b] Chemistry Department, College of Science, King Saud University, P.O. 2455, Riyadh 11451, Saudi Arabia
[c] Institute of Organic Chemistry and Technology, Faculty of Chemical Technology, University of Pardubice, Czech Republic
[d] Institute of Materials Chemistry, Brno University of Technology, Czech Republic
[e] Chemistry Department, Faculty of Science, Damanhour University, Damanhour, Egypt
[f] Chemistry Department, Faculty of Science, Fayoum University, Fayoum, Egypt
[g] Textile Research Division, National Research Center, Dokki, P.O. 12622, Giza 12522, Egypt

ARTICLE INFO

Article history:
Received 17 October 2013
Received in revised form 1 November 2013
Accepted 26 November 2013
Available online 4 December 2013

Keywords:
Green synthesis
Silver nanoparticles
Schizophyllan
Cytotoxicity

ABSTRACT

Silver nanoparticles (Ag-NPs) have been successfully prepared with a simple and "green" chemical reduction method. Triple helical schizophyllan (SPG) was used for the first time as reducing and stabilizing agents. The effect of temperature, silver nitrate/schizophyllan concentrations, pH of the reactions medium and the reaction time were investigated. The obtained schizophyllan/Ag-NP was characterized by UV–vis spectroscopy, TEM, DLS, X-ray diffraction, TGA, and ATR-FTIR. The results revealed that, Ag-NPs attached to SPG through a strong non-covalent interaction, leading to good dispersion of Ag-NPs with a diameter of 6 nm within the biopolymer matrix. By increasing the pH of the reaction medium, the triple helical structure of SPG was partially broken. The SPG/AgNP nanocomposite was non-toxic for mouse fibroblast line (NIH-3T3) and human keratinocyte cell line (HaCaT).

1. Introduction

Metal nanoparticles and their polymer composites represent an important field for fundamental studies offering wide range of engineering and biomedical applications. Due to the large surface area of common nanoparticles (NPs), controlled dispersion of NPs in the matrix remains one of the main difficulties. When the NPs were used alone, they showed strong aggregation resulting in a significant reduction of their surface activity (Zhu et al., 2002). To reduce the NP aggregation, preparation of nanoparticle compounds, in which individual NPs are distributed within the suitable polymer matrix, is one of the most effective approaches (Choy, Park, & Yoon, 1998; Miao et al., 2006; Mogyorósi, Dékány, & Fendler, 2003).

Natural polymers such as sodium hyaluronante (Abdel-Mohsen, Hrdina, et al., 2012; Abdel-Mohsen et al., 2013), chitosan and/or chitosan derivatives (Abdel-Mohsen, Abdel-Rahman, et al., 2012; Abdel-Mohsen, Aly, Hrdina, & El-Aref, 2012; Fouda, El-Aassar, & Al-Deyab, 2013), and cellulose are all important macromolecular materials increasingly used in biomedical applications due to their inherent biodegradability with degradation products which is non-toxic for the cells.

There are several methods for preparation of metal and metal oxide nanoparticles, such as photo-chemical reduction (Darroudi, Ahmad, Shameli, Abdullah, & Ibrahim, 2009), laser libations (Darroudi et al., 2011), chemical reduction with different polymers/biopolymers (Aihara, Torigoe, & Esumi, 1998; El-Rafie et al., 2011; Lin, Teng, & Yang, 2003), reduction of chemicals in soft and stiff matrices (Darroudi, Ahmad, Abdullah, Ibrahim, & Shameli, 2010; Hebeish, El-Rafie, Abdel-Mohdy, Abdel-Halim, & Emam, 2010; Zhuang, Cheng, Kang, & Xu, 2010) reduction of chemicals in staple matrices (e.g., porous silicate) (Dag, Samarskaya, Coombs, & Ozin, 2003), and chemical deposition (Szłyk et al., 2001; Textor, Fouda, & Mahltig, 2010).

Environmentally friendly (green) way to prepare silver nanoparticles (Ag-NPs) depend on three important parameters, such as solvent medium, reducing and stabilizing or capping agent for Ag-NPs (Abdel-Mohsen, Hrdina, et al., 2012; Hebeish et al., 2011). Many methods reported to use external reducing agents for preparation of silver nanoparticles. The use of toxic or harmful reducing

* Corresponding author at: Central European Institute of Technology (CEITEC), Brno University of Technology, Czech Republic. Tel.: +420 773063837.
** Corresponding author at: Chemistry Department, College of Science, King Saud University, P.O. 2455, Riyadh 11451, Saudi Arabia. Tel.: +966 560773127.
E-mail addresses: abdel-mohsen@ceitec.vutbr.cz, abdo_mohsennrc@yahoo.com (A.M. Abdel-Mohsen), m_gaballa@yahoo.com, mmfoudah@ksu.edu.sa (M.M.G. Fouda).

0144-8617/$ – see front matter © 2013 Elsevier Ltd. All rights reserved.
http://dx.doi.org/10.1016/j.carbpol.2013.11.040

agent, such as sodium borohydride, results in tiny particles that are well-dispersed (Ji, Chen, Wai, & Fulton, 1999; Shah, Holmes, Doty, Johnston, & Korgel, 2000). Nowadays, a succession chemical reduction method is used for the synthesis of noble metal nanoparticles such as, sodium borohydride (Shameli et al., 2010; Shen et al., 2010), ammonia solution (Lim, Jiang, Yu, Camargo, & Xia, 2010), diazine (Mayer, Grebner, & Wannemacher, 2000; Underhill & Liu, 2000), dimethyl aminoborane (Torigoe, Suzuki, & Esumi, 2001), hydrogen (Henglein & Giersig, 2000), HCHO, $HCONH_2$ (Yin et al., 2002), C_2H_5 (Wang, Neoh, & Kang, 2001; Wang, Ren, Deng, Gui, & Tang, 2000), $C_5H_5O_7Na$ (Pathak et al., 2000), and ascorbic acid (Lim et al., 2010). Schizophyllan (SPG), as biopolymer, is an extracellular linear β-1,3-glucan with one β-6-1-linked glucose residue per three main chain glucose residues produced by the fungus *Schizophyllum commune*. The chemical structure was shown in Fig. 1D-I. Norisuye and coworkers (Kashiwagi, Norisuye, & Fujita, 1981; Norisuye, 1985; Norisuye, Yanaki, & Fujita, 1980; Sato, Norisuye, & Fujita, 1981; Yanaki, Norisuye, & Fujita, 1980) studied the properties of schizophyllan biopolymer in details and they found that, SPG has triple helical structure shape, and the helical structure of SPG was stabilized by inter and/or intra hydrogen bonds among with the glucan chains in SPG, which are interconnected inside the helix, whereas one glucan residue per each repeating unit was directed outward the helix core into water as a solvent. The triple helical structure of SPG was found to be interacted in water even at 120 °C (Sato, Norisuye, & Fujita, 1983) and can be destroyed only in mixture of 85% DMSO/H_2O (Sato et al., 1983). Based on this finding; no structural transition above 10 °C in water was observed. In the present preparation method (SPG) was used, as the first time, for the preparation of silver nanoparticles (Ag-NPs), serving as reducing and capping agent for the formed Ag-NPs. Water was also utilized as the environmentally benign solvent throughout the preparation of Ag-NPs. The effect of reaction condition, including the pH value, temperature, and concentrations of both $AgNO_3$, SPG, and time on the size and morphology of AgNPs are discussed. Furthermore, the SPG/Ag-NPs nanocomposite structure was investigated employing TEM, X-ray diffraction, XRD, UV–vis spectra. The cytotoxicity of SPG/Ag-NPs nanocomposite was evaluated against NIH-3T3 and HaCaT cells.

2. Experimental

2.1. Materials

Schizophyllan extracted from *S. commune* weight (1.6 MDa, by SEC-MAALS) was purchased from CPN Ltd., Czech Republic. Sodium hydroxide and silver nitrate were obtained from Sigma–Aldrich, Germany. Deionized water was used for all experiments. All other solvents were used without further purification.

2.2. Methods

2.2.1. Preparation of silver nanoparticles by SPG

Desired amount of SPG was dissolved in 100 ml deionized water using heated magnetic stirrer and, after being completely dissolved, it was heated at reaction temperature ranging from 40 to 90 °C. The $AgNO_3$ solution with contraction ranging from 0.1 to 3 mg/ml was added drop-wise to the SPG solution (0.1–1%) under continuous stirring for 20–240 min. After adding the $AgNO_3$ solution, the SPG solution acquires light yellow color indicating the reduction of silver nitrate to Ag-NPs, after completing the reaction; the solution was centrifuged at 10,000 rpm for 15 min to remove the precipitate. The suspension of SPG/Ag-NP composite was then filtered through a 0.22 μm pore size filter paper followed by freeze-drying. To obtain the nanocomposite for the characterization, the SPG/Ag-NP was dissolved in deionized water (Millipore). Reaction conditions affecting the shape and size of Ag-NPs were studied and are discussed in the following section.

2.3. Characterization of schizophyllan–silver (SPG/Ag-NPs) nanoparticle composite

2.3.1. UV–visible (UV–vis) spectroscopy

UV–vis spectra measurement was carried out on UV-160A, Shimadzu, Japan) using quartz cuvettes with an optical path of 1 cm. The concentration of the measured solutions was kept at 0.4 mg/ml.

2.3.2. Transmission electron microscopy (TEM)

TEM images were observed on a JEOL JEM-2010 (HT) electron microscope, using an accelerating voltage of 150 kV. The sample was dissolved in deionized water (Millipore) with concentration of 0.4 mg/ml, and a drop was placed on Cu grids pre-coated with carbon films.

2.3.3. Dynamic light scattering (DLS)

Dynamic light scattering measurement was performed by a Malvern Zetasizer Nano ZS. The sample was filtered using a 0.45 μm nylon syringe filter directly into a polyacrylic cell.

2.3.4. X-ray diffraction (XRD)

XRD data were collected on a D8 Advance diffractometer (Bruker AXS, Germany) with Bragg–Brentano θ–θ goniometer (radius 217.5 mm) equipped with a secondary beam curved graphite mono-chromator and Na(Tl) I scintillation detector. The generator was operated at 40 kV and 30 mA. The scan was performed at room temperature from 10° to 80° (2θ) in 0.02° step with a counting time of 8 s per step.

2.3.5. Thermal analysis

The kinetics of thermal decomposition was investigated using different heating rate thermo-gravimetric (TG, Netzsch 209F3 instrument, Al_2O_3 crucible) and under heating rates of 5 °C min^{-1} (with data collecting rate of 40 points/K).

2.3.6. Attenuated total reflectance Fourier transforms infrared spectroscopy (ATR-FTIR)

Attenuated total reflectance Fourier transforms infrared spectroscopy (ATR-FTIR) spectroscopy was performed by using a Nicolet Impact 400 D FTIR spectrophotometer (Nicolet CZ, Prague, Czech Republic) equipped with a ZnSe crystal for the ATR-FTIR spectroscopy. Transmittance was measured as a function of the wave number between 4000 cm^{-1} and 600 cm^{-1} with the resolution of 8 cm^{-1} and the number of scans equal to 512.

2.3.7. Cell viability assay

As described by Vistejnova 2009 "3000 (3T3) and 4000 (HaCaT) cells/were seeded to 96-well test plates". "The cells were cultured for 24 h before treated with the cell solution". The tested solution was added to each well so that the final concentration of the tested solution in the well was 100–1000 μg/ml by diluent medium. Cytotoxicity was measured after 0, 24, 48, 72 h after the treatment with 3-(4.5-dimethylthiazol-2-yl)-2.5-diphenyl tetrazolium bromide assay. MTT is reduced by viable cells to a colored formazan salt, which the later released from the cells and determined spectrophotometrically. MTT assay was described in previously work (Vistejnova et al., 2009).

Also described by Vistejnova et al., 2009 "MTT stock solutions were added to the cell culture medium/plates were incubated at 37 °C for 2.5 h. The supernatant was discarded and cells were lysed

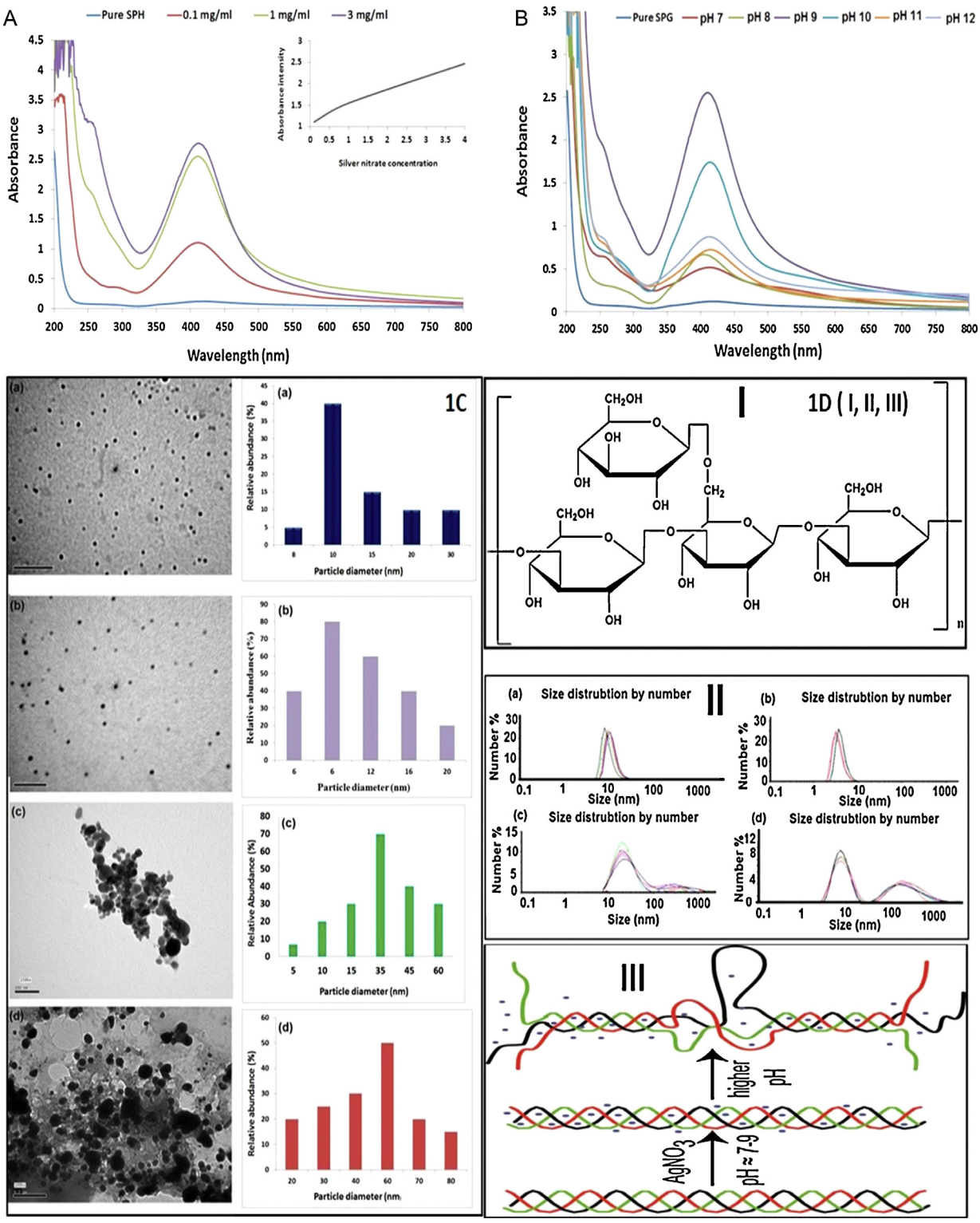

Fig. 1. (A) Effect of silver nitrate concentration on the preparation of nanocomposite. *Reaction conditions*: pH 9; reaction time, 1 h; SPG concentration, 1%; temperature, 90 °C. (B) Effect of pH on the preparation of SPG/Ag-NPS nanocomposite. *Experimental conditions*: SPG concentration, 1%; duration time, 1 h; reaction temperature, 90 °C; $AgNO_3$ concentration, 1 mg/ml. (C) TEM of silver–schizophyllan nanocomposite prepared at different pH (a) 7, (b) 9, (c) 10 and (d) 12. *Experimental conditions*: SPG concentration, 1%; duration time, 1 h; reaction temperature, 90 °C; $AgNO_3$ concentration, 1 mg/ml. (D-I) Chemical structure of schizophyllan (SPG). (D-II) DLS of schizophyllan/silver nanocomposite prepared at different pHs. *Experimental conditions*: (a) pH 7, (b) pH 9, (c) pH 10 and (d) pH 12. (D-III) The interaction proposed of silver nanoparticles before and after destruction of triple helical structure of schizophyllan.

in lysis solution for 30 min on a shaker. The optical density was measured in 96-well plate by a versamax microplate reader (Molecular Devices, CA, USA) at a wavelength of 570 nm".

(NIH-3T3) Mouse fibroblast cell line (Sigma–Aldrich) was cultured till 20th passage. Cells of 5th–20th passage were used in the following experiments. NIH-3T3 was grown in with 3-(4.5-dimethylthiazol-2-yl)-2.5-diphenyl tetrazolium bromide assay supplemented with 10% phosphate buffer solution, glutamine (0.3 mg/ml), penicillin (100 μ/ml) and streptomycin (0.1 mg/ml) in 7.5% carbon dioxide at 37 °C in 75 cm^2 culture

flask as recommended by the supplier. Spontaneously immortalized human keratinocyte cell line (HaCaT) was grown in with 3-(4.5-dimethylthiazol-2-yl)-2.5-diphenyl tetrazolium bromide assay supplemented with 10% phosphate buffer solution, glutamine, and gentamycin in 5% carbon dioxide at 37 °C. HaCaT cells were seeded overnight one day before the all experimental treatments.

SPG/Ag-NPs nanocomposite solution was prepared using cell cultivation medium to obtained concentrations from 100 to 1000 μg/ml, and filtrated (0.22 μm). The solution was added to each well so that the final concentration of the tested solution in the well was 100–1000 μg/ml using as diluent medium.

The experiments were carried out at least in four independent repeats. The Student's *t* test for two samples was applied to evaluate statistical importance of the results considering $p \leq 0.05$ significant. IFS Services statistical tests on-line service was utilized.

3. Results and discussion

3.1. Preparation of silver nanoparticles using schizophyllan (SPG)

Deionized water was used as the solvent for dissolution of the silver nitrate and SPG, and SPG was used as capping and stabilizing agent for the formed Ag-NPs in order to prevent their agglomeration in the reaction mixture. The SPG was used as in situ reducing agent for the Ag ions.

3.1.1. Preparation of schizophyllan–silver nanocomposite (SPG/Ag-NPs)

There are many parameters effecting the preparation of Ag-NPs, such as the silver nitrate and SPG concentrations, reaction time and temperature and solution pH controlling the size of the Ag-NPs as well as the homogeneity of the particle distributions.

3.1.2. Effect of silver nitrate concentration

At first, the effect of silver nitrate concentration on the preparation of nanocomposite (SPG/Ag-NPS) was studied. Fig. 1A shows UV–vis spectroscopy of the different concentration of silver nitrate (0.1–3 mg/ml) which affect the preparation of nanocomposite (SPG/Ag-NPs). As described below, the three peaks exhibited the same maximum absorption at approximately 412 nm which confirm the formation of silver nanoparticles. By increasing the concentration of silver nitrate, the intensity of the new beak at approximately 412 nm increased as well. This can be attributed to the overlap occurred with silver nanoparticles. The maximum absorbance of silver displays liner correlation by increasing the Ag-NPs concentration, as shown in the right side of Fig. 1A. On increasing the silver nanoparticles content, the intensity of the maximum absorbance increased linearly.

3.1.3. Effect of pH on the preparation of (SPG/Ag-NPs) nanocomposite

As mentioned above, SPG can be transformed from triple helical structure to random coil chains under alkaline condition, which accelerate the aggregation of AgNPs (Wang et al., 2010). Fig. 1B shows the UV–vis spectra for reactions carried out at different pH and its effect on the Ag^+ reduction. Below pH 7.0, there is no peak related to silver nanoparticles. Only a single broad peak related to silver ion nanoparticle appears at pH 7, corresponding to the existence of silver nanoparticle clusters. With increasing the pH from 7 to 9, a new absorbance band appeared at about 400–420 nm, suggesting the formation of Ag nanoparticles. The intensity of the band increased proportionally to the pH within this interval. Further increase of the pH of the reaction medium to 10–12, resulted in a decrease of the intensity of the absorption band proportional to the increase of the pH value. In addition, the higher the pH the higher the reduction rate of Ag^+.

3.1.4. Transmission electron microscopy and histogram of nanocomposite prepared at different pH values

It is obviously found in Fig. 1C that, the maximum absorption peak intensity increases gradually by increasing the pH value of the reaction medium until pH 9. But there is another phenomenon start to appear at higher pH, where the triple helical structure of schizophyllan convert to mono helical one, this phenomenon confirmed by using TEM and DLS techniques (Fig. 1C-c, d and D-II). By increasing the pH to a higher value more than 9, there were some aggregation of metal nanoparticles as shown by TEM in addition, localized surface plasmon (Fig. 1C-c and d) resonance (LSPR) decreased as described by UV–vis. The LSPR spectra of metal nanoparticles is highly depending on the size, shape and surrounding environment (Huang & Xu, 2010), specifically the aggregation phenomenon of metal and metal oxide nanoparticles through electrostatic force, van der walls, or bridge interactions (Wang, Tejerina, Lagzi, Kowalczyk, & Grzybowski, 2010) could influence the LSPR. This can be clearly explains the possible change of the size, shape, and environment of the schizophyllan–Ag nanocomposite. To investigate this change of SPG–Ag solution under higher pH, TEM images were recorded under different pHs.

Fig. 1C shows TEM pictures of SPG/Ag-NPs that prepared at different pH (Fig. 1C-a and b). From TEM, and histogram of nanocomposite prepared at pH 7 and 9, respectively, there is no any aggregation or agglomeration of silver nanoparticles and from the histogram shown in (Fig. 1C-a and b) and the particle size of silver nanoparticles was approximately between 6 and 10 nm. By increasing the pH values from 10 to 12; aggregations of silver nanoparticles occur as described in the histogram (Fig. 1C-c and d). The distance between Ag^0 nanoparticles became shorter; in addition, clear increasing in the density and concentration of silver nanoparticles in the bulk area occurred at higher pH, as shown in Fig. 1C-c and d. Fig. 1D-I shows the chemical structure of schizophyllan triple helical, schizophyllan macromolecules that may allow guest molecules to penetrate into their inner spaces (Kashiwagi et al., 1981; Yanaki et al., 1980). The data in figure (ID-IIa–d) show the dynamic light scattering of schizophyllan/silver nanocomposite at different pH (7–10). As described in figure ID-IIa, at pH 8, only one sharp beak appear at 10 ± 2 nm) which is related to silver nanoparticles described by TEM in (Fig. 1C-a). Also schizophyllan/silver nanocomposite prepared at pH 9 had very well dispersion with particle size ±2 nm and only one beak appear which is related to silver nanoparticles.

On increasing the pH of the reaction medium from 10 to 12, there are two beaks appear one of them at 10–100 (related to silver nanoparticles) and second one is broad at 100–1000 nm (related to the triple helical structure of schizophyllan that been converted to random coil structure), and by increasing the pH more than 11, the intensity of the second beak, which was related to the random coil of schizophyllan, increases as well as the intensity of the first beak of silver nanoparticles decrease due to some aggregation and agglomeration of silver nanoparticles. The data was also confirmed by TEM (Fig. 1C-d and e).

From the TEM and DLS analysis of SPG/Ag-NP nanocomposite, we proposed the SPG exhibits transition from triple helical to random coil structure with increasing the reaction mixture pH (Fig. 1D-III).

3.1.5. Effect of reaction time on nanocomposite preparation

Fig. 2A shows the UV–vis absorption spectra of Ag-NP colloidal solutions prepared from 1% of SPG with 1 ml of $AgNO_3$ solution (1 mg/ml) at 90 °C for different reaction times. A weak absorption band appeared at approximately 410 nm after 20 min in the

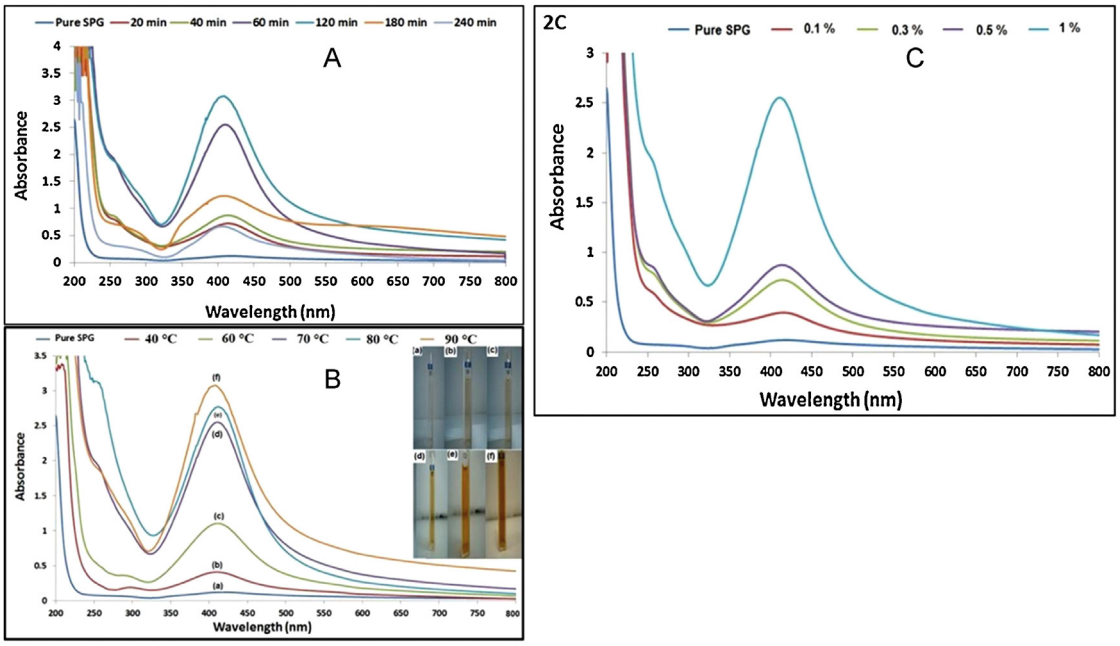

Fig. 2. (A) Effect of duration time on preparation of silver nanoparticles. *Reaction conditions*: SPG concentration, 1%; $AgNO_3$ concentration, 1 mg/ml; temperature, 90 °C; pH 9. (B) Effect of temperature on the preparation of nanocomposite. *Reaction conditions*: SPG concentration, 1%; $AgNO_3$ concentration, 1 mg/ml; duration time, 1 h; pH 9. (C) UV–vis absorption spectra for the SPG/Ag-NPs prepared by different concentration of schizophyllan. *Reaction conditions*: $AgNO_3$ concentration, 1 mg/ml; temperature, 90 °C; pH 9; duration time, 1 h.

reaction. This band became significantly more pronounced after 30 min in the reaction, suggesting the presence of spherical Ag-NPs in the system (Jradi et al., 2010). The absorption peak intensity increased rapidly with increasing the reaction time up to 2 h due to the continual formation of Ag-NPs in the reaction mixture. However, further increase of the reaction time from 180 to 240 min resulted in a decrease of the absorption peak intensity for the silver nanoparticles. The peak appearing after 180 and 240 min was asymmetrical and showed no absorption from 430 nm to 600 nm, thus, indicating that negligible aggregation occurred in this reactive system under the conditions investigated (Chen, Wang, Zhang, & Jin, 2008). Meanwhile, the color of the SPG–$AgNO_3$ solution changed from colorless to yellow, further indicating the formation of Ag-NPs.

3.1.6. Effect of temperature on the reaction condition

Fig. 2B shows the effect of reaction temperature on the reduction of silver ions to silver nanoparticles as illustrated by UV–vis spectroscopy. It is well know that, an absorption band appear at 400–430 nm which is related to surface plasmon resonance of silver nanoparticles (Abdel-Mohsen, Aly, et al., 2012). Here, no band appears at this region for pure schizophyllan at 40 °C. Only this band starts to appear by increasing the temperature of the reaction from 40 to 90 °C. Yellow solution was appearing with the appearance of absorption band at 410 nm on UV–vis spectra, suggestion the formation of silver nanoparticles. The spectra of the sample reacted at 90 °C for 1 h had the higher absorption intensity (at about 410 nm) than the other reacted at 40 °C. The result suggest, that silver ion reduction is strongly depends on the reaction temperature, and at higher reaction temperature, a higher reaction temperature causes higher reduction rate of silver ions to silver nanoparticles Ag^+ to Ag^0. In the right side of Fig. 2B, the photos of pure schizophyllan (a), schizophyllan/silver nanocomposite prepared at different temperature (b–f), where the change of color from colorless (pure schizophyllan, a) in the left side to yellowish (schizophyllan/silver nanocomposite, b–f) in relation to reaction temperature is described.

3.1.7. Effect of schizophyllan (SPG) concentration

Fig. 2C shows the UV–vis spectra of the Ag-NPs prepared with different concentrations of SPG (0.1–1%) and 1 mg/ml of $AgNO_3$ at 90 °C for 1 h. At lower SPG concentration (0.1%) Ag ions were not totally reduced and capped for the preparation of Ag-NPs and from Fig. 2C appear shorter beak at 275 nm which is related to silver ions. By increasing the concentration of SPG from 0.1 mg/ml to 0.5%, the silver band appeared at approximately 412 nm, indicating the formation of Ag-NPs. When the concentration of SPG increased up to 1%, the absorption intensity increased and the shape of the absorption band for silver nanoparticle became much narrower compared with less concentration of SPG. Our results suggest that using SPG with concentration of 1% is sufficient for the synthesis of well-defined Ag-NPs. No Ag-NPs agglomerates were observed under these conditions.

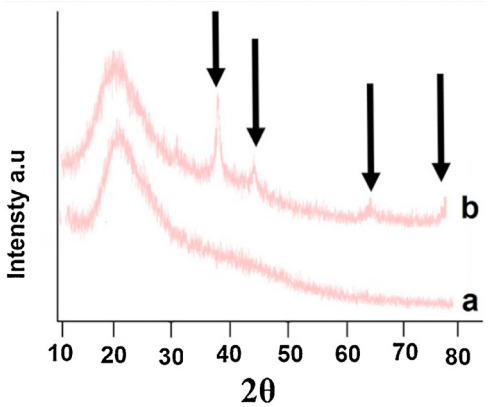

Fig. 3. XRD of (a) pure schizophyllan and (b) silver/schizophyllan nanocomposite. *Experimental conditions*: SPG concentration, 1%; $AgNO_3$ concentration, 1 mg/ml; duration time, 1 h; pH 9; temperature of reaction, 90 °C.

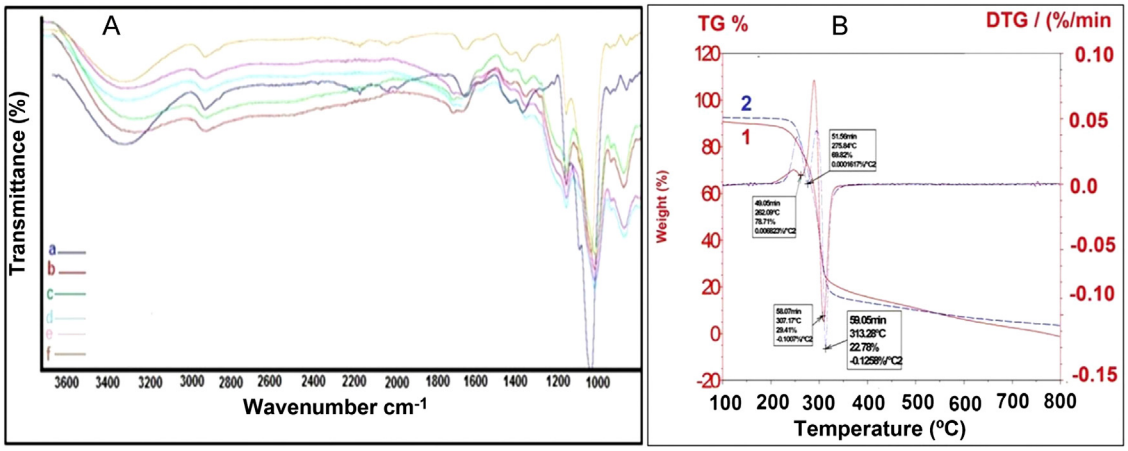

Fig. 4. (A) ATR-FTIR of schizophyllan/silver nanocomposite prepared by different concentration of silver nanoparticles. (a) Pure schizophyllan, (b) silver nanoparticles 0.1 mg/ml, (c) silver nanoparticles 0.3 mg/ml, (d) silver nanoparticles 0.5 mg/ml, (e) silver nanoparticles 1 mg/ml and (f) silver nanoparticles 3 mg/ml. *Experimental conditions*: SPG concentration, 1%; duration time, 1 h; pH 9; temperature of reaction, 90 °C. (B) TGA–DTG of pure schizophyllan, schizophyllan/silver nanocomposite (b). *Experimental conditions*: SPG concentration, 1%; $AgNO_3$ concentration, 1 mg/ml; duration time, 1 h; pH 9; reaction temperature, 90 °C.

3.2. XRD of silver/schizophyllan nanocomposite

Fig. 3 shows the X-ray diffraction (XRD) of pure schizophyllan and schizophyllan/silver nanocomposite prepared by chemical reduction method. The diffractogram of the pure SPG (Fig. 3a) exhibited only one broad beak at $2\theta = 19^\circ$ related to the schizophyllan. In Fig. 3b, four diffraction peaks were obtained, which were attributed to $2\theta = 39.4^\circ$, 44.6°, 63.5°, 78.1° corresponding to the (1 1 1), (2 0 0), (2 2 0) and (3 1 1) crystallographic planes of Ag°. These results indicated that silver nanoparticles formed in the schizophyllan matrix.

3.3. ATR-FTIR of schizophyllan/silver nanocomposite

Fig. 4A shows the ATR-FTIR spectra of the pure SPG and the SPG–Ag nanoparticles composites with different concentration of silver nanoparticles. The peaks at 3300–3450 cm^{-1} corresponded to the stretch vibrations of OH groups of the schizophyllan. As the concentration of Ag°, related to the increase of silver nitrate concentration (0.1–3 mg/ml), the shifted beak decreased to a lower value (Fig. 4A-b–f), this indicates the presence of strong interactions between the OH groups of SPG and the Ag-NPs. From FTIR data, the silver ions could be easily interact on the chains of

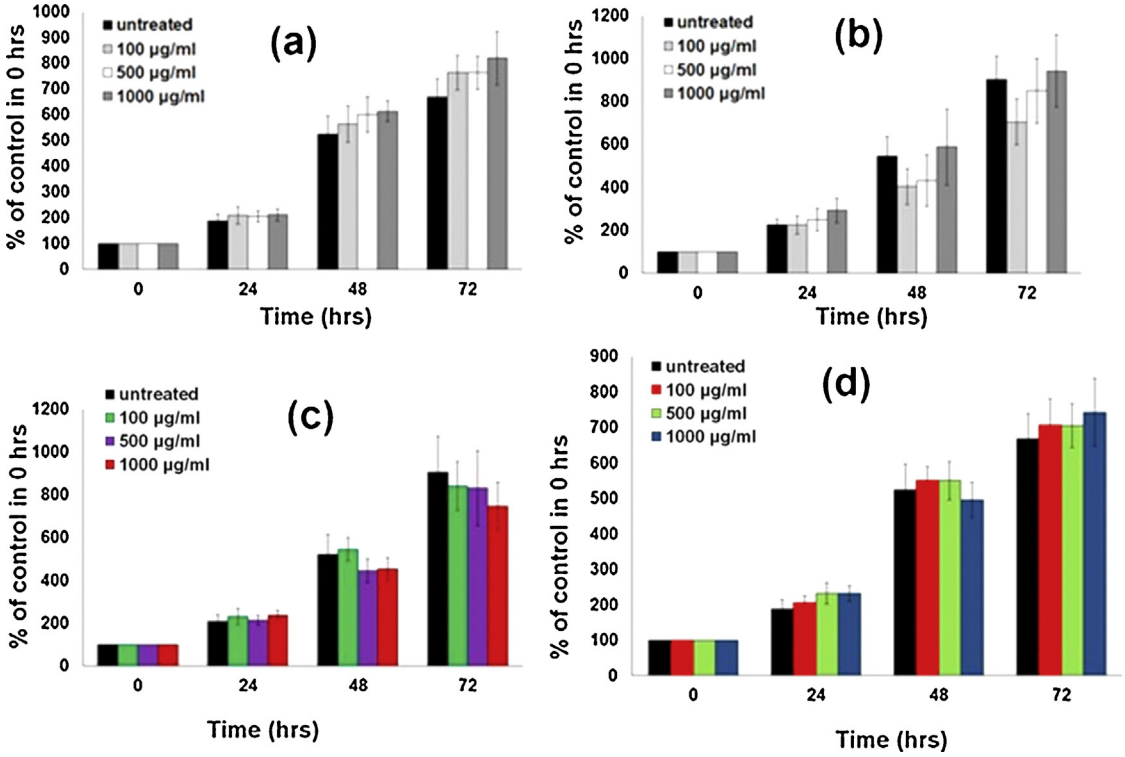

Fig. 5. Effect of pure schizophyllan, schizophyllan/silver nanocomposite on the cell viability of mouse fibroblast (NIH-3T3) and human keratinocyte (HaCaT) cell line. Cell viability was assessed at 0, 24, 48, and 72 h. (a) Pure schizophyllan (100–1000 μg/ml), 3T3 viability, MTT, $n = 6$, (b) schizophyllan/silver nanocomposite (100–1000 μg/ml), Ag-NPs (10 nm), 3T3 viability, MTT, $n = 6$, (c) pure schizophyllan (100–1000 μg/ml), HaCaT viability, MTT, $n = 6$, (d) schizophyllan/silver nanocomposite (100–1000 μg/ml), Ag-NPs (10 nm), HaCaT viability, MTT, $n = 6$.

the schizophyllan through electrostatic interactions. Moreover, the helical structure of schizophyllan absorbs Ag ions without any change. This highly stabilization or capping of silver nanoparticles in schizophyllan aqueous solution could be attributed to the electronegativity of the OH groups of schizophyllan, which strangely immobilized the metal ions. The non-covalent interaction between the polysaccharide and Ag was stronger than that between silver nanoparticles themselves.

3.4. Thermal stability of schizophyllan and silver/schizophyllan nanocomposite

Fig. 4B shows the thermograms (TGA–DTG) of schizophyllan (Fig. 4B-1) and the schizophyllan/silver nanocomposite (Fig. 4B-2). The thermograms that the thermal stability of schizophyllan/silver nanocomposite was different from that of pure schizophyllan, incorporation of silver nanoparticles in the matrix of schizophyllan shifted the onset of the thermal decomposition toward higher temperature. The thermal decomposition of pure schizophyllan was at 307 °C, and for nanocomposite was at 313 °C. At the same time, the thermograms indicate that the residual weight of schizophyllan/silver nanocomposite was almost higher than that of schizophyllan at 790 °C.

3.5. Cytotoxicity of SPG and SPG/Ag-NP nanocomposite

Fig. 5a and c shows the cytotoxicity of pure schizophyllan and schizophyllan/silver nanocomposite matrix with the mouse fibroblast (NIH-3T3) and Fig. 5b and c that of the human keratinocyte (HaCaT) cell lines. Fig. 5a shows the cell vitality in pure schizophyllan tested with mouse fibroblast (NIH-3T3) by using different concentrations (100–1000 μg/ml) after 24, 48, and 72 h exposition. The results suggest that the neat schizophyllan was non-toxic for mouse fibroblast cell line in the entire interval 0–72 h monitored. Similarly, the schizophyllan/silver nanocomposite did not exhibit any measurable toxicity for the mouse fibroblast (NIH-3T3) (Fig. 5b) over the concentration ranging from 100 to 1000 μg/ml after 24, 48 and 72 h of seeding the cells.

Fig. 5c shows the human keratinocyte cell (HaCaT) vitality in schizophyllan. The cells were seeded with different concentration of schizophyllan (100–1000 μg/ml) and different period time (24, 48, 72 h). Schizophyllan was non-toxic material for the human keratinocyte cells, the cells growth and proliferation occurred without any change compared to the reference system. In Fig. 5d, the human keratinocyte cell (HaCaT) vitality in the schizophyllan/silver nanocomposite is depicted. The schizophyllan/silver nanocomposite was non-toxic for human keratinocyte cells (HaCaT) for different concentrations (100–1000 μg/ml) of the nanocomposite at different exposure times (0, 24, 48, and 72). From all the cytotoxicity data, one can conclude that, there is no cytotoxicity effect of the new SPG/Ag-NP composite for mouse fibroblast (NIH-3T3) and human keratinocyte (HaCaT) cells over a wide range of temperature, concentration and exposition time.

4. Conclusions

Silver nanoparticles were prepared employing “green” chemistry by using schizophyllan as both reducing and stabilizing agent for the first time. The concentrations of silver nitrate and schizophyllan, reaction time and temperature and reaction mixture pH were varied broadly to obtain uniform and homogenous dispersion of silver nanoparticles. The formation of silver nanoparticles was monitored via color change which is confirmed by using the UV–vis spectra analysis, TEM, DLS, ATR-FTIR, TGA, and XRD. Results obtained conclude that schizophyllan/silver nanocomposite with the desired structure can be prepared using 1% schizophyllan, 1 mg/ml $AgNO_3$; at 90 °C and pH 9 after 60 min reaction time. The resulting Ag-NPs exhibited average size of (6 ± 2 nm) and were of spherical shape. The schizophyllan and SPG/Ag-NP nanocomposite were nontoxic over a wide range of concentrations (100–1000 μg/ml) and exposure lasting up to three days. The nanocomposite did not compromise either the vitality or growth of the fibroblasts or keratinocytes. We believe that schizophyllan/silver nanocomposite can be used for many biomedical applications especially for wound healing applications.

Acknowledgements

The authors would like to extend their sincere appreciation to the Deanship of Scientific Research at King Saud University for its funding of this research through the Research Group Project No. RGP-VPP-201.

This work was financially supported by the project “CEITEC – Central European Institute of Technology – excellent teams (CZ.1.07/2.3.00/30.0005)” financed from European Social Fund and (CZ.1.05/1.1.00/02.0068) from European Regional Development Fund.

References

Abdel-Mohsen, A. M., Abdel-Rahman, R. M., Hrdina, R., Imramovský, A., Burgert, L., & Aly, A. S. (2012). Antibacterial cotton fabrics treated with core–shell nanoparticles. *International Journal of Biological Macromolecules*, *50*(5), 1245–1253.

Abdel-Mohsen, A. M., Aly, A. S., Hrdina, R., & El-Aref, A. (2012). A novel method for the preparation of silver/chitosan-O-methoxy polyethylene glycol core shell nanoparticles. *Journal of Polymers and the Environment*, *20*(2), 459–468.

Abdel-Mohsen, A. M., Hrdina, R., Burgert, L., Abdel-Rahman, R. M., Hašová, M., Šmejkalová, D., et al. (2013). Antibacterial activity and cell viability of hyaluronan fiber with silver nanoparticles. *Carbohydrate Polymers*, *92*(2), 1177–1187.

Abdel-Mohsen, A. M., Hrdina, R., Burgert, L., Krylová, G., Abdel-Rahman, R. M., Krejčová, A., et al. (2012). Green synthesis of hyaluronan fibers with silver nanoparticles. *Carbohydrate Polymers*, *89*(2), 411–422.

Aihara, N., Torigoe, K., & Esumi, K. (1998). Preparation and characterization of gold and silver nanoparticles in layered laponite suspensions. *Langmuir*, *14*(17), 4945–4949.

Chen, J., Wang, J., Zhang, X., & Jin, Y. (2008). Microwave-assisted green synthesis of silver nanoparticles by carboxymethyl cellulose sodium and silver nitrate. *Materials Chemistry and Physics*, *108*(2–3), 421–424.

Choy, J.-H., Park, J.-H., & Yoon, J.-B. (1998). Multilayered SiO_2/TiO_2 nanosol particles in two-dimensional aluminosilicate catalyst–support. *The Journal of Physical Chemistry B*, *102*(31), 5991–5995.

Dag, O., Samarskaya, O., Coombs, N., & Ozin, G. A. (2003). The synthesis of mesostructured silica films and monoliths functionalised by noble metal nanoparticles. *Journal of Materials Chemistry*, *13*(2), 328–334.

Darroudi, M., Ahmad, M. B., Abdullah, A. H., Ibrahim, N. A., & Shameli, K. (2010). Effect of accelerator in green synthesis of silver nanoparticles. *International Journal of Molecular Sciences*, *11*, 3898–3905.

Darroudi, M., Ahmad, M. B., Shameli, K., Abdullah, A. H., & Ibrahim, N. A. (2009). Synthesis and characterization of UV-irradiated silver/montmorillonite nanocomposites. *Solid State Sciences*, *11*(9), 1621–1624.

Darroudi, M., Ahmad, M. B., Zamiri, R., Abdullah, A. H., Ibrahim, N. A., Shameli, K., et al. (2011). Preparation and characterization of gelatin mediated silver nanoparticles by laser ablation. *Journal of Alloys and Compounds*, *509*(4), 1301–1304.

El-Rafie, M. H., El-Naggar, M. E., Ramadan, M. A., Fouda, M. M. G., Al-Deyab, S. S., & Hebeish, A. (2011). Environmental synthesis of silver nanoparticles using hydroxypropyl starch and their characterization. *Carbohydrate Polymers*, *86*(2), 630–635.

Fouda, M. M. G., El-Aassar, M. R., & Al-Deyab, S. S. (2013). Antimicrobial activity of carboxymethyl chitosan/polyethylene oxide nanofibers embedded silver nanoparticles. *Carbohydrate Polymers*, *92*(2), 1012–1017.

Hebeish, A., El-Naggar, M. E., Fouda, M. M. G., Ramadan, M. A., Al-Deyab, S. S., & El-Rafie, M. H. (2011). Highly effective antibacterial textiles containing green synthesized silver nanoparticles. *Carbohydrate Polymers*, *86*(2), 936–940.

Hebeish, A. A., El-Rafie, M. H., Abdel-Mohdy, F. A., Abdel-Halim, E. S., & Emam, H. E. (2010). Carboxymethyl cellulose for green synthesis and stabilization of silver nanoparticles. *Carbohydrate Polymers*, *82*(3), 933–941.

Henglein, A., & Giersig, M. (2000). Reduction of Pt(II) by H_2: Effects of citrate and NaOH and reaction mechanism. *The Journal of Physical Chemistry B*, *104*(29), 6767–6772.

Huang, T., & Xu, X.-H. N. (2010). Synthesis and characterization of tunable rainbow colored colloidal silver nanoparticles using single-nanoparticle plasmonic microscopy and spectroscopy. *Journal of Materials Chemistry*, *20*(44), 9867–9876.

Ji, M., Chen, X., Wai, C. M., & Fulton, J. L. (1999). Synthesizing and dispersing silver nanoparticles in a water-in-supercritical carbon dioxide microemulsion. *Journal of the American Chemical Society*, *121*(11), 2631–2632.

Jradi, S., Balan, L., Zeng, X. H., Plain, J., Lougnot, D. J., & Royer, P. (2010). Spatially controlled synthesis of silver nanoparticles and nanowires by photosensitized reduction. *Nanotechnology*, *21*, 95605–95612.

Kashiwagi, Y., Norisuye, T., & Fujita, H. (1981). Triple helix of *Schizophyllum commune* polysaccharide in dilute solution. 4. Light scattering and viscosity in dilute aqueous sodium hydroxide. *Macromolecules*, *14*(5), 1220–1225.

Lim, B., Jiang, M., Yu, T., Camargo, P. C., & Xia, Y. (2010). Nucleation and growth mechanisms for Pd–Pt bimetallic nanodendrites and their electrocatalytic properties. *Nano Research*, *3*(2), 69–80.

Lin, X. Z., Teng, X., & Yang, H. (2003). Direct synthesis of narrowly dispersed silver nanoparticles using a single-source precursor. *Langmuir*, *19*(24), 10081–10085.

Mayer, A. B. R., Grebner, W., & Wannemacher, R. (2000). Preparation of silver–latex composites. *The Journal of Physical Chemistry B*, *104*(31), 7278–7285.

Miao, S., Liu, Z., Han, B., Zhang, J., Yu, X., Du, J., et al. (2006). Synthesis and characterization of TiO_2–montmorillonite nanocomposites and their application for removal of methylene blue. *Journal of Materials Chemistry*, *16*(6), 579–584.

Mogyorósi, K., Dékány, I., & Fendler, J. H. (2003). Preparation and characterization of clay mineral intercalated titanium dioxide nanoparticles. *Langmuir*, *19*(7), 2938–2946.

Norisuye, T. (1985). Triple-stranded helical structure of schizophyllan and its antitumor activity in aqueous solution. *Die Makromolekulare Chemie*, *14*(S19851), 105L 118.

Norisuye, T., Yanaki, T., & Fujita, H. (1980). Triple helix of a *Schizophyllum commune* polysaccharide in aqueous solution. *Journal of Polymer Science: Polymer Physics Edition*, *18*(3), 547–558.

Pathak, S., Greci, M. T., Kwong, R. C., Mercado, K., Prakash, G. K. S., Olah, G. A., et al. (2000). Synthesis and applications of palladium-coated poly(vinylpyridine) nanospheres. *Chemistry of Materials*, *12*(7), 1985–1989.

Sato, T., Norisuye, T., & Fujita, H. (1981). Melting behavior of *Schizophyllum commune* polysaccharides in mixtures of water and dimethyl sulfoxide. *Carbohydrate Research*, *95*(2), 195–203.

Sato, T., Norisuye, T., & Fujita, H. (1983). Triple helix of *Schizophyllum commune* polysaccharide in dilute solution. 5. Light scattering and refractometry in mixtures of water and dimethyl sulfoxide. *Macromolecules*, *16*(2), 185–189.

Shah, P. S., Holmes, J. D., Doty, R. C., Johnston, K. P., & Korgel, B. A. (2000). Steric stabilization of nanocrystals in supercritical CO_2 using fluorinated ligands. *Journal of the American Chemical Society*, *122*(17), 4245–4246.

Shameli, K., Ahmad, M. B., Zin Wan Yunus, W. M., Ibrahim, N. A., Rahman, R. A., Jokar, M., et al. (2010). Silver/poly (lactic acid) nanocomposites: Preparation, characterization, and antibacterial activity. *International Journal of Nanomedicine*, *5*, 573–579.

Shen, J., Shi, M., Li, N., Yan, B., Ma, H., Hu, Y., et al. (2010). Facile synthesis and application of Ag-chemically converted graphene nanocomposite. *Nano Research*, *3*(5), 339–349.

Szłyk, E., Piszczek, P., Grodzicki, A., Chaberski, M., Goliński, A., Szatkowski, J., et al. (2001). CVD of AgI complexes with tertiary phosphines and perfluorinated carboxylates—A new class of silver precursors. *Chemical Vapor Deposition*, *7*(3), 111–116.

Textor, T., Fouda, M. M. G., & Mahltig, B. (2010). Deposition of durable thin silver layers onto polyamides employing a heterogeneous Tollens' reaction. *Applied Surface Science*, *256*(8), 2337–2342.

Torigoe, K., Suzuki, A., & Esumi, K. (2001). Au(III)–PAMAM interaction and formation of Au–PAMAM nanocomposites in ethyl acetate. *Journal of Colloid and Interface Science*, *241*(2), 346–356.

Underhill, R. S., & Liu, G. (2000). Preparation and performance of Pd particles encapsulated in block copolymer nanospheres as a hydrogenation catalyst. *Chemistry of Materials*, *12*(12), 3633–3641.

Vistejnova, L., Dvorakova, J., Hasova, M., Muthny, T., Velebny, V., Soucek, K., et al. (2009). The comparison of impedance-based method of cell proliferation monitoring with commonly used metabolic-based techniques. *Neuro Endocrinology Letter*, *30*, 121–127.

Wang, D., Tejerina, B., Lagzi, I., Kowalczyk, B., & Grzybowski, B. A. (2010). Bridging interactions and selective nanoparticle aggregation mediated by monovalent cations. *ACS Nano*, *5*(1), 530–536.

Wang, J., Neoh, K. G., & Kang, E. T. (2001). Preparation of nanosized metallic particles in polyaniline. *Journal of Colloid and Interface Science*, *239*(1), 78–86.

Wang, Y., Ren, J., Deng, K., Gui, L., & Tang, Y. (2000). Preparation of tractable platinum, rhodium, and ruthenium nanoclusters with small particle size in organic media. *Chemistry of Materials*, *12*(6), 1622–1627.

Yanaki, T., Norisuye, T., & Fujita, H. (1980). Triple helix of *Schizophyllum commune* polysaccharide in dilute solution. 3. Hydrodynamic properties in water. *Macromolecules*, *13*(6), 1462–1466.

Yin, Y., Li, Z.-Y., Zhong, Z., Gates, B., Xia, Y., & Venkateswaran, S. (2002). Synthesis and characterization of stable aqueous dispersions of silver nanoparticles through the Tollens process. *Journal of Materials Chemistry*, *12*(3), 522–527.

Zhu, H. Y., Orthman, J. A., Li, J. Y., Zhao, J. C., Churchman, G. J., & Vansant, E. F. (2002). Novel composites of TiO_2 (anatase) and silicate nanoparticles. *Chemistry of Materials*, *14*(12), 5037–5044.

Zhuang, X., Cheng, B., Kang, W., & Xu, X. (2010). Electrospun chitosan/gelatin nanofibers containing silver nanoparticles. *Carbohydrate Polymers*, *82*(2), 524–527.